Chattering Eliminated and Stable Gait Planning of Biped Robots Using a Fuzzy Sliding Mode Controller

Amir Takhmar[1], Mansoor Alghooneh[2], S. Ali A. Moosavian[3]
1- Electrical and Computer Department, University of Western Ontario, London, ON, CAN;
Email: amir.takhmar@gmail.com
2- Mechanical and Manufacturing Department, University of Manitoba, Winnipeg, MB, CAN;
Email: alghooneh@gmail.com; + corresponding author;
3- Mechanical and Manufacturing Department, K. N. Toosi Univ. of Tech., Tehran, Iran;
Email: moosavian@kntu.ca.ir

Received: December 2011 Revised: July 2012 Accepted: October 2012

ABSTRACT:
Control of biped walking robots based on designated smooth and stable trajectories is a challenging problem that is the focus of this article. Because of highly nonlinear dynamics of biped robots, minor uncertainties in systems parameters may drastically affect the system performance, leading to a chattering phenomenon. To tackle this, a new Sliding Mode Control (SMC) approach is proposed privileging a chattering elimination method based on Fuzzy logic to regulate the switching gain. To this end, first a desired trajectory for the lower body will be designed to alleviate the impacts due to contact with the ground. This is obtained by fitting proper polynomials at appropriate break points. Then, the upper body motion is planned based on the Zero Moment Point (ZMP) criterion to provide a stable motion for the biped robot. Next, dynamics equations will be obtained for both single support phase (SSP) and double support phase (DSP). Finally, the SMC approach is applied for both the SSP and the DSP, while a new chattering elimination method using Fuzzy logic will be proposed based on regulating a constant switching gain. Obtained simulation results show that the performance of the system is properly accurate in terms of the tracking errors even in the presence of considerable uncertainties and exerted disturbances. Furthermore, the new proposed method substantially reduces chattering effects and avoids the instability of the biped robot due to this phenomenon, resulting in stable smooth motion control of this complicated system.

KEYWORDS: Biped Robots, Fuzzy Systems, Sliding Mode Control, Stability, Gait Planning.

1. INTRODUCTION

Control of biped robots requires appropriate gait planning that can generate smooth stable walking. One of the earliest criteria to investigate the stability of such systems is the *Zero Moment Point* (ZMP) criterion, [1-2]. The ZMP is a point where the horizontal components of the resultant moment of all external forces, including gravity and inertial forces, becomes zero. According to the ZMP criterion if that point is inside the *support polygon*, which is defined as the foot supporting surface on the ground, the robot will be stable; otherwise the robot will tend to tip over. Goswami has introduced the *Foot Rotation Indicator* (FRI) criterion [3-4]. The FRI corresponds with a point where the net ground reaction force would exert to keep the foot stationary. According to this criterion if the FRI point is inside the support polygon, the robot will be stable, otherwise the robot will tend to tip over. The FRI criterion has been introduced only for the single support phase (SSP). Various compensation methods have been also proposed that use the upper body motion to compensate the stability of the biped robots and yield stable gate planning [5-6]. Vukobratovic has used the prescribed synergy method to obtain the upper body motion [6]. According to the prescribed synergy method, the nonlinear differential equations for upper body motion are obtained and solved by iteration method, where the dynamics equations in single and double support phases are different. Because of complexity of equations of motion and short time of double support phase (DSP), most researchers have only investigated these robots in SSP [7-8]. However, when a biped robot walks with low speed, the effect of the DSP becomes more important.

To track planned trajectories by a biped robot, various control strategies have been suggested and implemented. These include linear control [9], Computed Torque Method (CTM) [10-11], adaptive control [12], and robust control [13-14]. One of the

most popular controllers is CTM that is a model-based controller, and requires perfect knowledge of the system dynamics. Therefore, the main disadvantage of CTM and similar algorithms is performance deterioration due to parameter uncertainties. Because of highly nonlinear dynamics of biped robots, minor uncertainties in systems parameters may drastically affect the system performance. To overcome this problem exploiting robust control strategies is recommended. Robust control strategy has low sensitivity to uncertainties such as parameter uncertainty, disturbances and unmodeled dynamics. Among different robust controllers, the Sliding Mode Control (SMC) is a suitable control approach that ensures good tracking performance despite parameter uncertainties. Both CTM and SMC have been applied for the single support phase (SSP) of a 5 DOF biped robot, where the SMC results in a better performance compared to CTM [7]. The SMC has been also applied for the double support phase (DSP) of a 5 DOF biped robot (without active feet) [13-14]. However, the SMC experiences chattering problem that is due to switching process. Chattering problem excites undesired flexible dynamics, and deteriorates the system performance [15]. Furthermore, because of unstable nature of biped robots, the chattering effects on the ZMP position may even cause instability. In order to alleviate the SMC chattering problem, various approaches have been proposed. A common solution is replacing discontinuous sign function by continuous saturation function in a thin boundary layer around the switching surface [15]. Choosing a thinner boundary layer, makes the controller more robust but chattering amplifies, while with a larger boundary layer, chattering alleviates but tracking error increases. To resolve this contradiction, varying boundary layer approach [16], and replacing discontinuous control low by PID-like structure [17] have been proposed. Furthermore, a regulating routine has been proposed to determine proper positive values for the coefficient of sliding condition [18-19]. Adding a low pass filter on the sliding mode controller command to the actuator [20-21], and using hybrid control strategies such as designing a neural SMC [22], or fuzzy SMC [23], have been also proposed. However, most of these hybrid control strategies are complex and require a great extent of mathematical computations.

In this paper, to alleviate the chattering phenomenon, a new method based on fuzzy logic will be proposed and applied to control a biped walking robot. To this end, smooth trajectories for both feet, and the hip joint will be designed. Using of inverse kinematics and trajectories of feet and hip joint, the joint angles for the lower body will be obtained. To fulfill the robot stability, trunk motion will be used, and the system will be modeled as an inverse pendulum. Therefore, with this simple model, the motion of system center of mass (CM) will be expressed by a linear deferential equation. Solving this equation, based on the desired ZMP as an input, the robot CM will be constrained to match this solution. Then, the upper body motion will be obtained such that the CM constraint will be satisfied. After designing trajectories of all joint, dynamic equations will be obtained for both the SSP and the DSP, and the SMC algorithm is applied to both phases. To alleviate the chattering phenomenon, a new method based on fuzzy logic will be proposed that regulates the switching gain. Obtained results show that the tracking errors of the proposed controller will be considerably small even with major uncertainties and exerted disturbances. Also, the new proposed method substantially reduces chattering effects and avoids the instability of the biped robot due to chattering.

2. TRAJECTORY PLANNING

2.1. Lower Body Motion

2.1.1. Applying the ZMP Criterion

As shown in Fig. 1, the considered biped robot has 6 Degrees of Freedom, DOF, defined by six joint angles $(\theta_1,...,\theta_5,\theta_0)$. To apply the ZMP criterion, it can be obtained, [1-2]:

$$X_{ZMP}=\frac{\sum_i m_i(\ddot{z}_i+g)x_i-\sum_i m_i\ddot{x}_i z_i-\sum_i \tau_i)_y}{\sum_i m_i(\ddot{z}_i+g)} \quad (1)$$

$$Y_{ZMP}=\frac{\sum_i m_i(\ddot{z}_i+g)y_i-\sum_i m_i\ddot{y}_i z_i+\sum_i \tau_i)_x}{\sum_i m_i(\ddot{z}_i+g)} \quad (2)$$

where vector $[x_i,y_i,z_i]$ denotes the position of the mass center of the link$\mathrm{i}$, $\mathrm{m_i}$ denotes its mass, x_{zmp} and Y_{zmp} denote the position of the ZMP point in the original coordinate system, and τ_i denotes inertial moment. As mentioned before, if the ZMP is inside the support polygon, the robot will be stable, otherwise the robot will tend to tip over. The ZMP criterion will be introduced to plan the upper body motion to fulfill stability requirements, which will be discussed in details in Section IV. Here, the trajectories for the hip and the foot are determined.

The trajectory planning is performed considering the two phases of motion; the SSP and the DSP (DSP). For a better understanding of how the robot walks; the robot's feet are introduced with the right foot and the left foot. Suppose that at the initial step, the right foot is the swing one, and the left foot is on the ground, as

shown in Fig. 2. So, the SSP starts when the toe of the right foot leaves the ground, and terminates when the heel of the right foot touches the ground. When this phase is completed, the left foot is still in contact with the ground. Therefore, when the heel of the right foot touches the ground, the DSP starts till leaving the ground by left foot. For continuous walking cycle, the role of the feet is changed and walking cycle will continue. Based on the above, the foot and the hip trajectories will be designed below.

2.1.2. Foot Trajectory

To obtain the path of both feet, $[X_{ankle}, Z_{ankle}, \theta_{ankle}]$ should be determined, where $X_{ankle} and\ Y_{ankle}$ denote the coordinates of the ankle position, and θ_{ankle} denotes the slope of the foot. The following break points will be used in the determination of the foot slope:

$$\theta_{ankle} = \begin{cases} 0 & t = kT_c \\ q_b & t = kT_c + T_d \\ q_e & t = (k+1)T_c \\ 0 & t = (k+1)T_c + T_d \end{cases} \quad (3)$$

Then, horizontal and vertical foot positions can be written as:

$$X_{ankle} = \begin{cases} (k-1)D_s & t = kT_c \\ (k-1)D_s + b_2(1-\cos(q_b)) & t = kT_c + T_d \\ (k-1)D_s + X_{\max} & t = kT_c + T_{\max} \\ (k+1)D_s - b_1(1-\cos(q_e)) & t = (k+1)T_c \\ (k+1)D_s & t = (k+1)T_c + T_d \end{cases} \quad (4)$$

$$Z_{ankle} = \begin{cases} 0 & t = kT_c \\ -b_2 \sin(q_b) & t = kT_c + T_d \\ Z_{\max} & t = kT_c + T_{\max} \\ b_1 \sin(q_e) & t = (k+1)T_c \\ 0 & t = (k+1)T_c + T_d \end{cases} \quad (5)$$

where, $T_{\max}$ is the time that the ankle joint reaches to its maximum position in vertical direction. With these break points the robot is capable to pass any encountered obstacle. To alleviate the impact due to contact with the ground, the velocity of the foot is near zero when the toe of the foot leaves and the heel of the foot touches the ground. So, $\dot{\theta}_{ankle}$, $\dot{X}_{ankle} and\ \dot{Z}_{ankle}$ are taken equal to zero at $t = kT_c$ and $t = (k+1)T_c + T_d$. A fourth order polynomial will be used for above break points.

2.1.3. Hip Trajectory

The required hip break points are determined as follows:

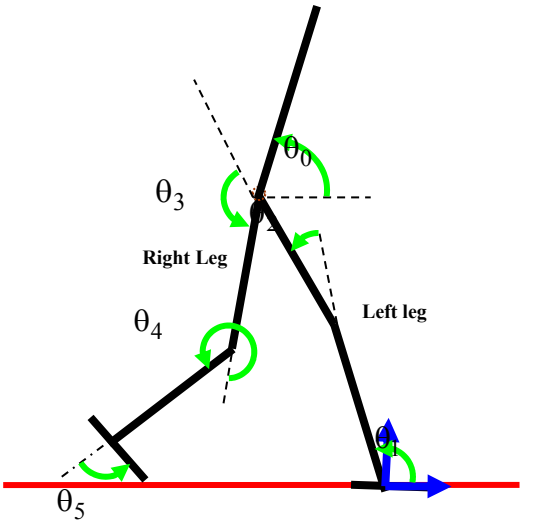

Fig.1. A 6 DOF biped robot.

$$X_{hip} = \begin{cases} (k-1)D_s + D_{ed} & t = kT_c \\ kD_s - D_{sd} & t = kT_c + T_d \\ kD_s + D_{ed} & t = (k+1)T_c \end{cases} \quad (6)$$

$$Z_{hip} = const \qquad kT_c < t < (k+1)T_c \quad (7)$$

Furthermore in order to obtain a smooth periodic hip motion, the following condition is imposed:

$$\begin{cases} \dot{X}_{hip}(kT_c) = \dot{X}_{hip}((k+1)T_c) \\ \ddot{X}_{hip}(kT_c) = \ddot{X}_{hip}((k+1)T_c) \end{cases} \quad (8)$$

Therefore, using a fourth order polynomial for successive break points, the hip motion will be determined. By determining the paths for the feet and the hip, trajectories for the robot lower body is complete, and based on the inverse kinematics solution; the joint angles will be determined.

2.2. Inverse Kinematics

To determine the joint angles, the inverse kinematics equations for both phases, i.e. SSP and DSP, are obtained in this section.

2.2.1. The Inverse Kinematics for the SSP

The joint angles $\theta = (\theta_1, \theta_2, \theta_3, \theta_4, \theta_5)$ will be determined using the paths of the swing foot $X_{a-r} = (x_a, z_a, \theta_a)$ and the hip $[X_{hip}, Z_{hip}]$ in the SSP. As shown in Fig. 1, the origin of the coordinate system is taken from the ankle joint of the left contacting foot. The position of the hip joint is written as:

$$\begin{aligned} x_{hip} &= l_1 \cos(\theta_1) + l_2 \cos(\theta_1 + \theta_2) \\ z_{hip} &= l_1 \sin(\theta_1) + l_2 \sin(\theta_1 + \theta_2) \end{aligned} \quad (9)$$

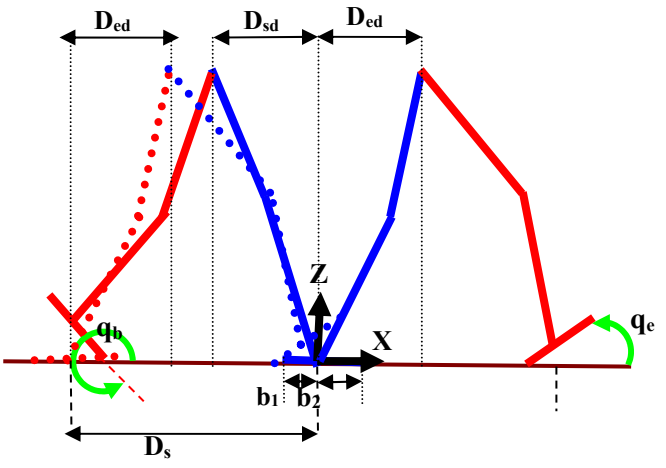

Fig. 2. Basic parameters of trajectory

Based on the recent equations, the value of θ_1 and θ_2 are determined as follows:

$$\theta_1 = -\cos^{-1}(B)+\alpha$$
$$B = \frac{A}{2x_{hip}\ l_1}\cos(\alpha) \quad (10)$$

$$\begin{cases} A = l_1^{\,2} - l_2^{\,2} + x_{hip}^{\,2} + z_{hip} \\ \alpha = \tan^{-1}\left(\dfrac{z_{hip}}{x_{hip}}\right) \end{cases} \quad (11)$$

$$\begin{cases} \theta_2 = a\tan 2(D,C) - \theta_1 \\ D = \dfrac{z_{hip} - l_1\sin(\theta_1)}{l_2} \\ C = \dfrac{x_{hip} - l_1\cos(\theta_1)}{l_2} \end{cases} \quad (12)$$

For determining the other joint's variables, the position of the right foot's ankle with respect to the original coordinate is written as follows:

$$x_a = x_{hip} + l_3\cos(\theta_1+\theta_2+\theta_3) + l_4\cos(\theta_1+\theta_2+\theta_3+\theta_4) \quad (13)$$

$$z_a = z_{hip} + l_3\sin(\theta_1+\theta_2+\theta_3) + l_4\sin(\theta_1+\theta_2+\theta_3+\theta_4) \quad (14)$$

$$\theta_a = \theta_1+\theta_2+\theta_3+\theta_4+\theta_5 \quad (15)$$

Based on equations (13)-(15), the values of θ_3, θ_4 and θ_5 can be obtained:

$$\begin{cases} \theta_3 = -\theta_1-\theta_2+\gamma-\cos^{-1}(H) \\ H = \dfrac{G\cos(\gamma)}{2El_3},\ G = E^2+F^2+l_3^{\,2}+l_4 \\ \gamma = \tan^{-1}\left(\dfrac{F}{E}\right)\ \ where\ \ E = x_a - x_{hip},\ \ F = z_a - z_{hip} \end{cases} \quad (16)$$

$$\begin{cases} \theta_4 = a\tan 2(J,I) - \theta_1 - \theta_2 - \theta_3 \\ I = \dfrac{x_a - x_{hip} - l_3\cos(\theta_1+\theta_2+\theta_3)}{l_4} \\ J = \dfrac{z_a - z_{hip} - l_3\sin(\theta_1+\theta_2+\theta_3)}{l_4} \end{cases} \quad (17)$$

$$\theta_5 = \theta_a - \theta_1 - \theta_2 - \theta_3 - \theta_4 \quad (18)$$

2.2.2. The Inverse Kinematics for the DSP

As shown in Fig. 3, in this phase based on the planned paths for the hip joint $X_{hip} = (x_{hip}, z_{hip})$ and the feet $X_{ankleleft} = (x_{a-l}, z_{a-l}, \theta_{a-l})$, $X_{ankle\ right} = (x_{a-r}, z_{a-r}, \theta_{a-r})$, the joint angles can be obtained. To this end, it can be written:

$$x_{hip} = b_2(1-\cos(\phi_1)) + l_1\cos(\phi_1+\theta_1) + l_2\cos(\phi_1+\theta_1+\theta_2) \quad (19)$$

$$z_{hip} = -b_2\sin(\phi_1) + l_1\sin(\phi_1+\theta_1) + l_2\sin(\phi_1+\theta_1+\theta_2) \quad (20)$$

In the above equations, ϕ_1 is equal to θ_{a-l} that is known. Therefore, θ_1 and θ_2 can be obtained as follows:

$$\begin{cases} \theta_1 = \alpha - \cos^{-1}(C) - \phi_1 \\ C = \dfrac{A^2+B^2+l_1^{\,2}-l_2^{\,2}}{2l_1A}\cos(\alpha),\ \ \alpha = \tan^{-1}\dfrac{B}{A} \end{cases} \quad (21)$$

$$\begin{cases} A = x_{hip} - b_2(1-\cos(\phi_1)) \\ B = z_{hip} + b_2\sin(\phi_1) \end{cases} \quad (22)$$

$$\begin{cases} \theta_2 = a\tan 2(F,E) - \phi_1 - \theta_1 \\ F = \dfrac{B - l_1\sin(\phi_1+\theta_1)}{l_2},\ and\ \ E = \dfrac{A - l_1\cos(\phi_1+\theta_1)}{l_2} \end{cases} \quad (23)$$

To determine other joint angles, the position of the right foot ankle is written as follows:

$$x_{a-r} = x_{hip} + l_3\cos(\phi_1+\theta_1+\theta_2+\theta_3) + l_4\cos(\phi_1+\theta_1+\theta_2+\theta_3+\theta_4) \quad (24)$$

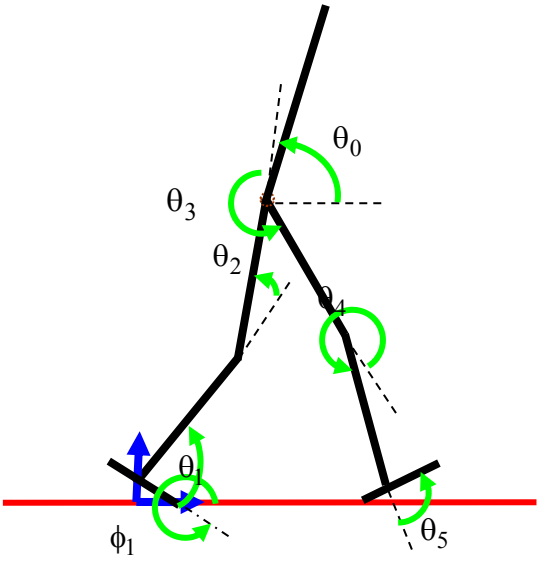

Fig. 3. The biped robot in DSP.

$$z_{a-r} = z_{hip} + l_3 \sin(\phi_1 + \theta_1 + \theta_2 + \theta_3) + l_4 \sin(\phi_1 + \theta_1 + \theta_2 + \theta_3 + \theta_4) \quad (25)$$

$$\theta_{a-r} = \phi_1 + \theta_1 + \theta_2 + \theta_3 + \theta_4 + \theta_5 \quad (26)$$

Then, based on these equations, values of θ_3, θ_4 and θ_5 will be obtained as:

$$\begin{cases} \theta_3 = \gamma - \cos^{-1}(J) - \phi_1 - \theta_1 - \theta_2 \\ J = \dfrac{I}{G}\cos\gamma, \quad I = \dfrac{G^2 + H^2 + {l_3}^2 - {l_4}^2}{2l_3} \\ \gamma = \tan^{-1}\dfrac{H}{G}, H = z_{a-r} - z_{hip}, \quad G = x_{a-r} - x_{hip} \end{cases} \quad (27)$$

$$\begin{cases} \theta_4 = a\tan 2(L, K) - \phi_1 - \theta_1 - \theta_2 - \theta_3 \\ L = \dfrac{H - l_3 \sin(\phi_1 + \theta_1 + \theta_2 + \theta_3)}{l_4} \\ K = \dfrac{G - l_3 \cos(\phi_1 + \theta_1 + \theta_2 + \theta_3)}{l_4} \end{cases} \quad (28)$$

$$\theta_5 = \theta_{a-r} - \phi_1 - \theta_1 - \theta_2 - \theta_3 - \theta_4 \quad (29)$$

Finally, the following condition is imposed to resume the next cycle:

$$\begin{aligned} &\theta_{1-NEW} = \pi - \theta_{5\_OLD} \quad , \theta_{2\_NEW} = -\theta_{4\_OLD} \\ &\theta_{3\_NEW} = 2\pi - \theta_{3\_OLD} \quad , \theta_{4\_NEW} = -\theta_{2\_OLD} \\ &\theta_{5\_NEW} = \pi - \theta_{1\_OLD} \end{aligned} \quad (30)$$

2.3. Upper Body Motion

In determining the lower body motion, the stability of the biped robot was not taken into account. So, the motion of the upper body will be determined for the compensation of robot's stability. To this end, the biped robot is modeled as an inverse pendulum shown in Fig. 4. To obtain the equation of motion for the inverse pendulum model, its height is assumed to be constant and since the motion of the robot is considered in the vertical plane, the equation of motion will be obtained as follows:

$$\ddot{X}_{CM} = \frac{g}{Z_{CM}}(X_{CM} - X_{ZMP}) \quad (31)$$

where X_{CM} and Z_{CM} denote the position of robot mass center and X_{ZMP} denotes the x-component of the robot's ZMP position. In fact, X_{CM} is determined at the beginning and the end of each walking cycle and Eq. (31) will be solved for the desired X_{ZMP}. Eq. (31) is a two boundary value problem and is solved based on Linear Shooting Method, [24].

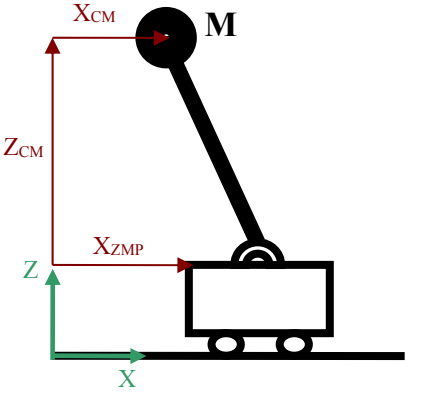

Fig. 4. The inverse pendulum model.

Therefore, the position of the robot's mass center will be obtained at each walking cycle, and then the obtained constraint is satisfied by the upper body motion as follows:

$$X_{CM} = \frac{\sum_{i=0}^{4} m_i x_i}{\sum_{i=0}^{4} m_i} \Rightarrow$$

$$x_0(\theta_{Trunk}) = \frac{X_{CM}\sum_{i=0}^{4} m_i + \sum_{i=1}^{4} m_i x_i}{m_0} \quad (32)$$

where the mass of feet was neglected and m_i denotes the mass of links 0 to 4 and x_i denotes the position of center of mass of links 0 to 4 as defined in Fig. 1.

Therefore, solving Eq. (32) at each step, the upper body motion will be obtained.

3. Dynamic Modeling

The biped robots exhibit different dynamics behavior in single and double support phases. In this section, the equations of motion for the considered robot will be developed for both phases.

3.1. Dynamics Equations in the SSP

According to Fig. 1, the generalized coordinates and generalized forces for the considered biped robot is obtained as follows:

$$\begin{aligned} q &= [\theta_1, \theta_2, \theta_3, \theta_4, \theta_5, \theta_0] \\ \tau &= [\tau_1, \tau_2, \tau_3, \tau_4, \tau_5, \tau_0] \end{aligned} \tag{33}$$

where τ_0 denotes the trunk torque, τ_1 and τ_2 denote the right leg joint torques, τ_3 and τ_4 denote the left leg joint torques, and τ_5 denotes the right (supporting) foot torque. The robot has 6 DOF in the SSP and the general form of dynamics equations in this phase is obtained as follows:

$$M_{6\times6}(q)\ \ \ddot{q} + C_{6\times6}(q,\dot{q})\dot{q} + G_{6\times1}(q) = \tau_{6\times1} \tag{34}$$

3.2. Dynamics Equations in the DSP

Two constraints are added to the considered biped robot in the DSP, since horizontal and vertical distances between the heel of the right foot and tip of the left foot should be taken as constant. Thus, the equations of motion in the DSP are different from the SSP. According to Fig. 3, the generalized coordinates and generalized forces in the DSP are defined as follows:

$$\begin{aligned} q &= [\phi_1, \theta_1, \theta_2, \theta_3, \theta_4, \theta_5, \theta_0] \\ \tau &= [\tau_{\phi_1}, \tau_1, \tau_2, \tau_3, \tau_4, \tau_5, \tau_0] \end{aligned} \tag{35}$$

where τ_{ϕ_1} denotes the left foot torque that its actuator is set on ankle joint, and the rest are as defined before. In Eq. (35), the vector of generalized coordinates is a 7×1 vector and as mentioned before in this phase two constraints are added, so the robot has 5 DOF in this phase. The constraints are as follows:

$$\begin{aligned} &-b_2\cos(\phi_1) + l_1\cos(\phi_1+\theta_1) \\ &+ l_2\cos(\phi_1+\theta_1+\theta_2) \\ &+ l_3\cos(\phi_1+\theta_1+\theta_2+\theta_3) + \ldots \\ &l_4\cos(\phi_1+\theta_1+\theta_2+\theta_3+\theta_4) \\ &-b_1\cos(\phi_1+\theta_1+\theta_2+\theta_3+\theta_4+\theta_5) = k_1 \end{aligned} \tag{36a}$$

$$\begin{aligned} &-b_2\sin(\phi_1) + l_1\sin(\phi_1+\theta_1) \\ &+ l_2\sin(\phi_1+\theta_1+\theta_2) \\ &+ l_3\sin(\phi_1+\theta_1+\theta_2+\theta_3) + \ldots \\ &l_4\sin(\phi_1+\theta_1+\theta_2+\theta_3+\theta_4) \\ &-b_1\sin(\phi_1+\theta_1+\theta_2+\theta_3+\theta_4+\theta_5) = k_2 \end{aligned} \tag{36b}$$

where k_1 and k_2 are constants. Differentiating from the above equations, the results can be written in the following form:

$$A^T\dot{q} = 0 \tag{37}$$

where A is a 7×2 vector. Adding these constraints to the previous equations, the dynamics model in the DSP is obtained as follows:

$$M_{7\times7}(q)\ \ \ddot{q} + C_{7\times7}(q,\dot{q})\dot{q} + G_{7\times1}(q) = \tau_{7\times1} + A_{7\times2}\lambda_{2\times1} \tag{38}$$

where λ denotes Lagrange multipliers. Solving Eqs. (38) requires solving Eqs. (38) simultaneously, which is not an easy task. Therefore, elimination of Lagrange multipliers from Eqs. (38) would be a proper solving strategy. To this end, the Natural Orthogonal Complement Method can be used, [25]. To use this method, a set of independent coordinates is defined as follows:

$$\beta = [\phi_1, \theta_1, \theta_2, \theta_3, \theta_0] \tag{39}$$

which can be related to the generalized coordinates as follows:

$$\dot{q}_{7\times1} = \Psi(q)\dot{\beta}_{5\times1} \tag{40}$$

Substituting Eq. (40) into Eq. (37), it can be obtained:

$$A^T\dot{q} = 0 \rightarrow A^T\Psi\dot{\beta} = 0 \xrightarrow{\dot{\beta}\neq0} A^T\Psi = 0 \ \ or \ \ \Psi^T A = 0 \tag{41}$$

Therefore, multiplying Eq. (38) by Ψ^T and making required simplifications, the dynamics equations of the considered biped robot in the DSP can be obtained as follows:

$$\begin{aligned} &\hat{M}_{5\times5}(q)\ \ \ddot{\beta} + \hat{C}_{5\times5}(q,\dot{q})\ \ \dot{\beta} + \hat{G}_{5\times1}(q) = \hat{\tau}_{5\times1} \\ &\hat{M} = \Psi^T M(q)\Psi,\ \ \hat{C} = \Psi^T M(q)\dot{\Psi} + \Psi^T C(q,\dot{q})\Psi \\ &\hat{G} = \Psi^T G(q),\ \ \hat{\tau} = \Psi^T\tau \end{aligned} \tag{42}$$

4. Sliding Mode Controller

In this section, a sliding mode controller is developed for both the SSP and the DSP. The objective is to determine an input τ such that in the presence of uncertainties, the state $Q = [q, \dot{q}]$ track the desired values $Q_d = [q_d, \dot{q}_d]$. The sliding surface or switching function for the biped robot is proposed to be described by:

$$s(Q,t)=\left(\frac{d}{dt}+\Lambda\right)^2\int_0^t\tilde{q}(T)dT=\dot{\tilde{q}}+2\Lambda\tilde{q}(T)+\Lambda^2\int_0^t\tilde{q}(T)dT \quad (43)$$

where $\tilde{q}=q-q_d$ defines the tracking error, Λ is an $n\times n$ diagonal matrix with selected positive constants, and "n" is the size of q (in the SSP $n=6$, and in the DSP $n=5$). It should be noted that we can interpret $s(Q,t)$ as velocity error:

$$s(Q,t)=\dot{q}-\dot{q}_r \quad (44a)$$

where,

$$\dot{q}_r=\dot{q}_d-2\Lambda\tilde{q}-\Lambda^2\int_0^t\tilde{q}(T)dT \quad (44b)$$

Substituting the dynamics model into $\dot{s}(Q,t)=0$, an equivalent control input τ_{eq} can be obtained by solving this equation. So, if the dynamics were exactly known, it can be written:

$$\dot{s}(Q,t)=\frac{d}{dt}s(Q,t)=\ddot{q}-\ddot{q}_r=0 \quad (45)$$

Which yields:

$$\tau_{eq}=\hat{M}(q)\ddot{q}_r+\hat{C}(q,\dot{q})\dot{q}_r+\hat{g}(q) \quad (46)$$

Where M, C *and* g describe the real robot dynamics, $\hat{M}$, $\hat{C}$ *and* $\hat{g}$ are the derived model and $\tilde{M}=\hat{M}-M$, $\tilde{C}=\hat{C}-C$, $\tilde{g}=\hat{g}-g$ describe the modeling errors.

The sliding mode control law is designed as:

$$\tau=\tau_{eq}-K\,\mathrm{sgn}(s) \quad (47a)$$

where K is an $n\times n$ diagonal matrix:

$$K=diag(k_1,k_2,...,k_i,...,k_n) \quad (47b)$$

and k_i's can be determined by using *Lyapunov's stability theorems*. A Lyapunov function candidate is chosen as a positive definite function:

$$V=\frac{1}{2}\mathbf{s}^{\mathrm{T}}\mathbf{M}\mathbf{s} \quad (48)$$

By differentiating of Lyapunov function, it is obtained:

$$\dot{V}=s^T\left(\tilde{M}(q)\ddot{q}_r+\tilde{C}(q,\dot{q})\dot{q}_r+\tilde{g}(q)-K\,\mathrm{sgn}(s)\right)+\frac{1}{2}s^T(\dot{M}(q)-2C(q,\dot{q}))s \quad (49a)$$

Where

$$\dot{q}^T(\tau-g(q))=\frac{1}{2}\frac{d}{dt}\left[\dot{q}^TM(q)\dot{q}\right]=\dot{q}^TM(q)\ddot{q}+\frac{1}{2}\dot{q}^T\dot{M}(q)\dot{q}$$

$$\dot{q}^T(\tau-g(q))=\frac{1}{2}\frac{d}{dt}\left[\dot{q}^TM(q)\dot{q}\right]=\dot{q}^TM(q)\ddot{q}+\frac{1}{2}\dot{q}^T\dot{M}(q)\dot{q} \quad (49b)$$

$$\Rightarrow\dot{q}^T(\tau-g(q))=\dot{q}^T(\tau-C(q,\dot{q})\dot{q}-g(q))+\frac{1}{2}\dot{q}^T\dot{M}\dot{q}$$

$$\Rightarrow\dot{q}^T\left(\dot{M}(q)-2C(q,\dot{q})\right)\dot{q}=0$$

Therefore:

$$\dot{V}=s^T\left(\tilde{M}(q)\ddot{q}_r+\tilde{C}(q,\dot{q})\dot{q}_r+\tilde{g}(q)-K\,\mathrm{sgn}(s)\right) \quad (50)$$

In order to guarantee that $\dot{V}\le-\eta|s|$ (a negative definite function), where η is a $n\times1$ vector with selected positive elements, the following condition must be hold:

$$k_i\ge\left|\tilde{M}(q)\ddot{q}_r+\tilde{C}(q,\dot{q})\dot{q}_r+\tilde{g}(q)\right|_i+\eta_i \quad (51)$$

In general, one of the problems with the SMC is the chattering phenomenon due to switching process, which may deteriorate the system performance, and cause instability. In fact, it can be observed that discontinuous function $\mathrm{sgn}(s)$ in the sliding control law of Eq. (47) could be a main source of chattering. To eliminate chattering, it has been proposed to smoothen this discontinuity in a narrow layer around the sliding surface, [15]:

$$B(t)=\left\{\ \tilde{Q}\middle|s(Q,t)\right|\le\phi_b,\ \ \phi_b>0\right\} \quad (52)$$

where ϕ_b is the boundary layer thickness. Therefore, the term $\mathrm{sgn}(s)$ is replaced by $sat(\frac{s}{\phi_b})$ that is defined as:

$$sat\left(\frac{s}{\phi_b}\right)=\begin{cases}1 & s>\phi_b\\ \dfrac{s}{\phi_b} & |s|<\phi_b\\ -1 & s<\phi_b\end{cases} \quad (53)$$

It should be noted that choosing a thinner boundary layer, makes the controller more robust but chattering amplifies, while with a larger boundary layer, chattering alleviates but tracking error increases. So, there is a contradiction between tracking performance and chattering characteristics.

The other main cause of chattering is using of a constant gain around the sliding surface, i.e. K in Eq. (47). Based on Eq. (51), usually the gain k_i is greater than η_i, and greater uncertainties require greater gains.

On the other hand, higher values of η_i causes chattering, while lower values lead to longer transient time. So, η_i should be selected such that (i) the stability holds, (ii) the system response time becomes reasonable, and (iii) chattering gets alleviated. A strategy to achieve these goals is that, when the distance from sliding surface increases, making η positively big enough to make the system move back to the sliding surface, and accordingly when the distance from sliding surface reduces, [18-19]. Based on this strategy, a fuzzy regulator is proposed next.

5. Regulating η Parameter with Fuzzy Logic

In this section, the η parameter is regulated as output of a fuzzy system, [26], as depicted in Fig. 5. The input to the system is $S=[s_1,s_2,...,s_n]^T$, where in case of the SSP $n=6$, and in the DSP $n=5$. The Membership Functions (MF) for the input are defined as shown in Fig. 6, in which ϕ is the boundary layer thickness. As seen, the Fuzzy sets of input are NBB, NB, NM, NS, NSS, Z, PSS, PS, PM, PB, PBB. Here, N, Z, and P denote negative, zero, and positive, respectively, B stands for big and BB for bigger than big, M is medium, S stands for small, and SS for smaller than small. The triangular MFs are chosen for NB, NM, NS, NSS, Z, PSS, PS, PM and PB, linear S shape for PBB, and linear Z shape for NBB. The output of the fuzzy system is $\eta=[\eta_1,\eta_2,...,\eta_n]^T$, that are defined in a normalized domain [0 1]. As shown in Fig. 7, the fuzzy sets of output are Z, PSS, PS, PM, PB, PBB.

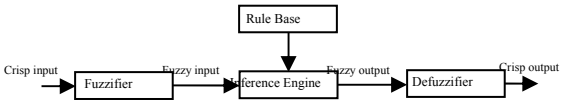

Fig. 5. Components of the fuzzy system

To alleviate chattering, as pointed in previous section, when the distance from sliding surface increases, one should make η positively big enough to make the system move back to the sliding surface, and accordingly when the distance from sliding surface reduces. Fuzzy rules that assure this trend are presented in Table 1.

6. Obtained Simulation Results

For the system depicted in Fig. 1, all geometric, mass and gait parameters are given in Table 2, while controller parameters are introduced in Table 3. Fig. 9 shows the designed trajectories for the ankle. As mentioned before, the trajectory for the lower body is designed to obtain a smooth motion with no impact due to contact with the ground. As shown in Fig. 9, the

Table 1. Fuzzy rules

Rule	1	2	3	4	5	6	7	8	9	10	11
s_i	NBB	NB	NM	NS	NSS	Z	PSS	PS	PM	PB	PBB
η_i	PBB	PB	PM	PS	PSS	Z	PSS	PS	PM	PB	PBB

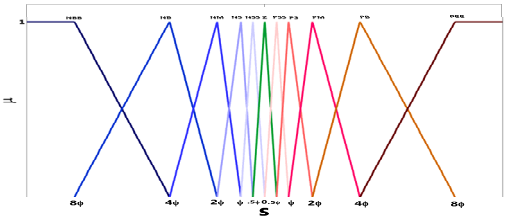

Fig. 6. Input fuzzy sets.

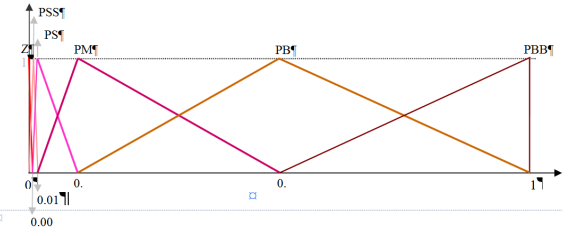

Fig. 7. Output fuzzy sets

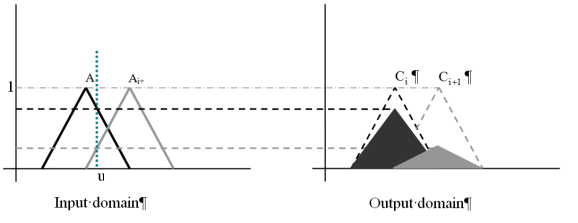

Fig. 8. Inference system using product max

Table 2. Geometric, mass and gait parameters

Masses (kg)	M_0 10	M_1 1	M_2 1	M_3 1	M_4 1
Mass Moments of Inertia ($kg.m^2$)	I_0 0.208	I_1 0.021	I_2 0.021	I_3 0.021	I_4 0.021
Lengths (m)	L_0 0.5	L_1(m) 0.5	L_2(m) 0.5	L_3(m) 0.5	L_4(m) 0.5
Gait Parameters (Fig. 2)	D_s(m) 0.15	b_1(m) 0.05	b_2(m) 0.15	q_e(rad) 0.262	q_b(rad) -0.262
	D_{ed}(m) 0.15	D_{sd}(m) 0.11	T_s(s) 3.5	T_d(s) 0.7	T_{max}(s) 1.9
	X_{max}(m) 0.25	Z_{max}(m) 0.10			

velocity of the foot is zero at the start, and end part of its vertical motion, and using inverse kinematics, trajectory for the joint angles of lower body is completed based on the feet and hip trajectories. Then, stability compensation is obtained by trunk motion. Thus, using of the moving ZMP in Eq. (31), the motion of CM is obtained. It should be mentioned that since the trunk link has maximum mass, the CM position of this link affects the position of the robot CM. An animated view of the robot motion is shown in Fig. 10.

Next, application of the ordinary sliding mode controller is investigated during both phases, i.e. the SSP and the DSP. The trajectory tracking errors and the ZMP variation are shown in Fig. 11 by using the proposed SMC without regulating η. As it can be seen, the system experiences a highly chattering response, which causes growth in trajectory tracking errors, particularly during DSP.

Next, the trajectory tracking error and the ZMP variation are shown in Fig. 12 by using the proposed SMC with Fuzzy regulated η. As can be seen in these figures by using the proposed regulating method the chattering is avoided and the ZMP tracking error vanishes in a short period. Also, tracking errors for joint angles remain acceptably small, converging to zero within the walking cycle. It should be mentioned that the response of the system remains almost similar to these illustrations for considerable uncertainties of up to 100 percent higher than real parameters.

To investigate the disturbance rejection characteristics of the proposed Fuzzy SMC, a constant 20 (N) force is exerted on the hip joint of the biped robot. It should be mentioned that the required joint torques during previous investigations are in the order of 10 (N.m). As can be seen in Fig. 13, the proposed controller can successfully control the stability of the robot with confined vanishing errors. Finally, as shown in part (d) of this figure, the reaction forces on contacting feet is acceptably enough to avoid sliding on surfaces with ordinary coefficients of friction.

6. Conclusions

This paper proposed a Sliding Mode Control approach with a new chattering elimination method using Fuzzy logic to regulate the switching gain. First, smooth trajectories for both feet, and the hip joint were designed. Then, using inverse kinematics, the joint angles for the lower body were obtained. To fulfill the robot stability, trunk motion was used, where the system was modeled as an inverse pendulum. Therefore, with this simple model, the motion of system center of mass (CM) was expressed by a linear deferential equation. Solving this equation, based on the desired ZMP as an input, the robot CM was constrained to coincide this solution. Then the upper body motion was obtained such that CM constraint was satisfied. After designing trajectories of all joint,

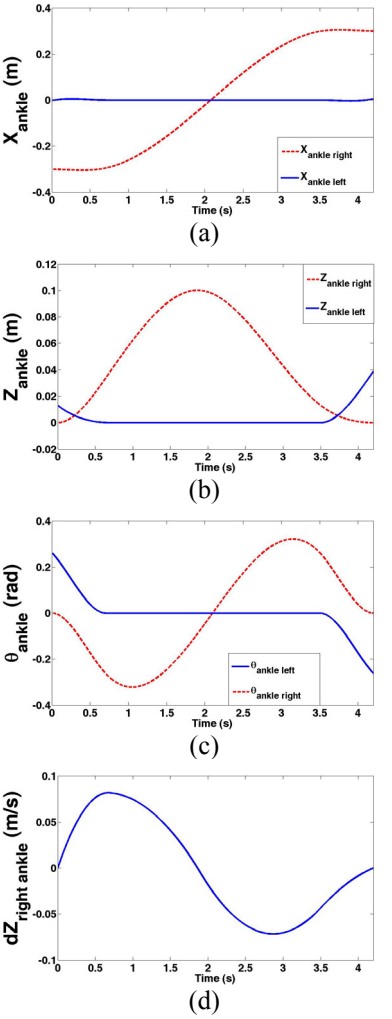

Fig. 9. Planned trajectories for the ankle joint: (a) x position, (b) z position, (c) Orientation (joint angle), (d) Vertical speed.

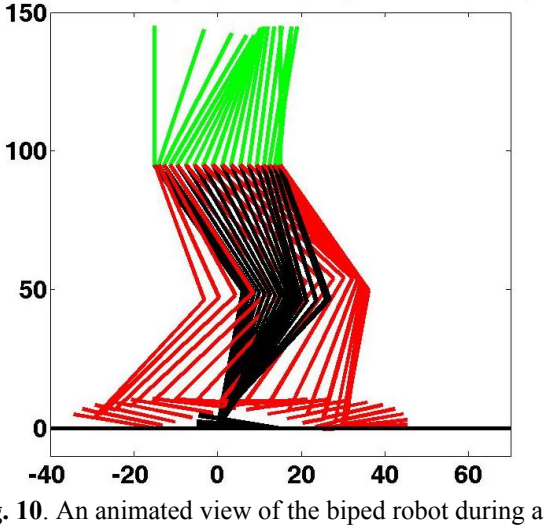

Fig. 10. An animated view of the biped robot during a walking cycle (SSP and DSP).

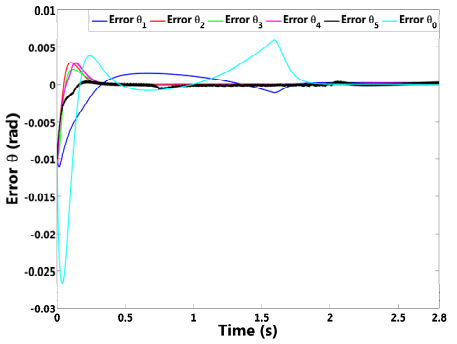

(a)

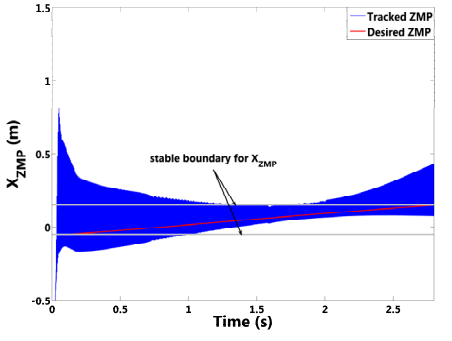

(b)

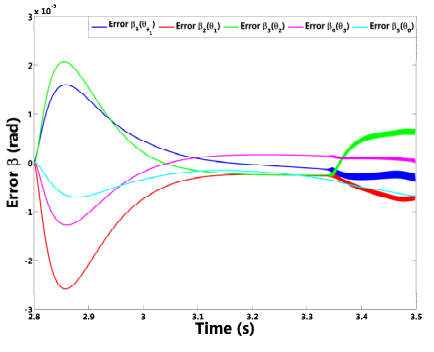

(c)

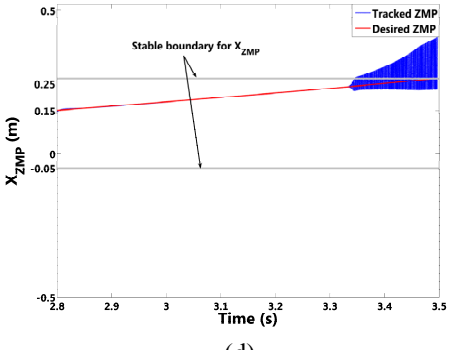

(d)

Fig. 11. Performance of ordinary SMC with constant η; (a) Joint angles tracking errors in the SSP, (b) The ZMP variation in the SSP, (c) Joint angles tracking errors in the DSP, (d) The ZMP variation in the DSP.

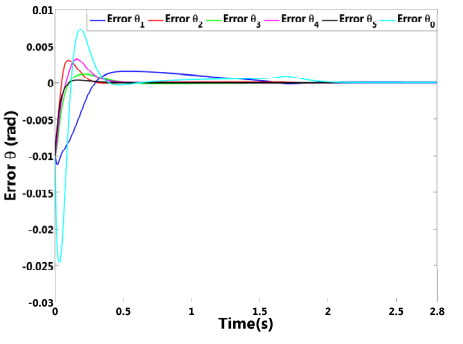

(a)

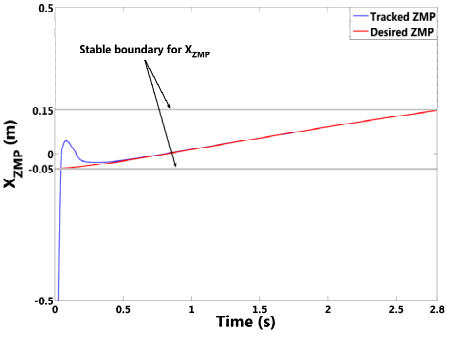

(b)

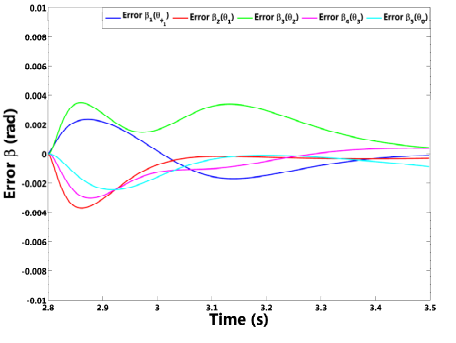

(c)

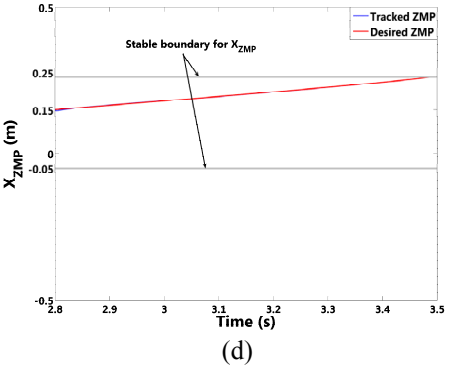

(d)

Fig. 12. Performance of the proposed Fuzzy SMC with regulated η; (a) Joint angles tracking errors in the SSP, (b) The ZMP variation in the SSP, (c) Joint angles tracking errors in the DSP, (d) The ZMP variation in the DSP.

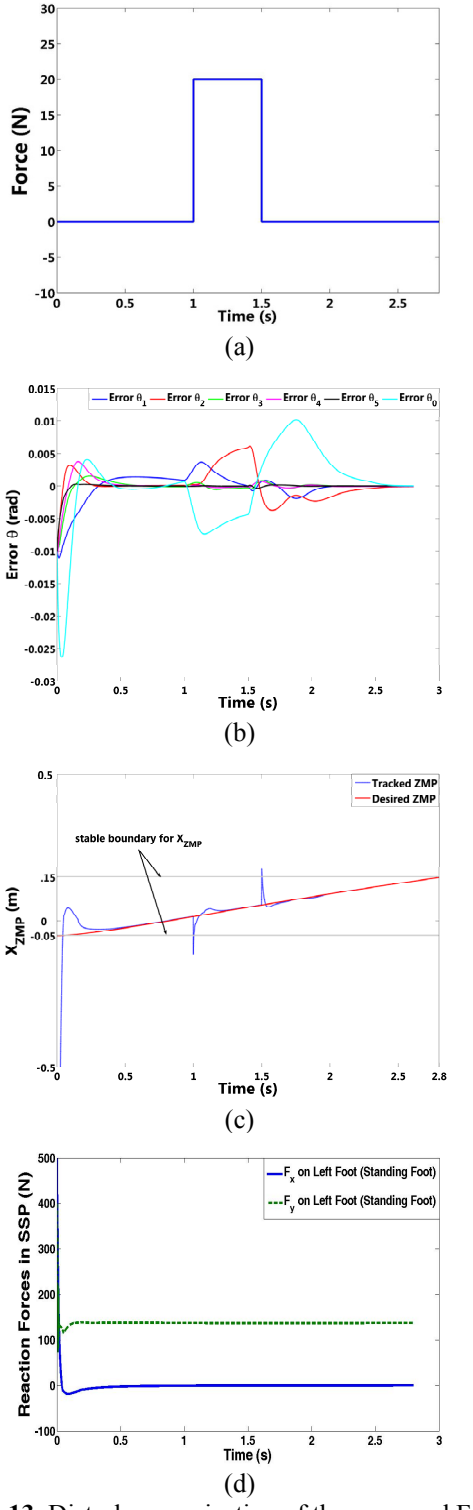

Fig. 13. Disturbance rejection of the proposed Fuzzy SMC with regulated η; (a) The disturbance force, (b) Joint angles tracking errors in the SSP, (c) The ZMP variation in the SSP, (d) The reaction forces in the SSP.

dynamic equations were obtained for both the SSP and the DSP, and the SMC algorithm was applied to both phases. To alleviate the chattering phenomenon, a new method based on fuzzy logic was proposed to regulate constant switching gain. Obtained results show that the tracking errors of the proposed controller were considerably small even with major uncertainties and exerted disturbances. Furthermore, the new proposed method substantially reduced chattering effects and avoided the instability of the biped robot due to chattering.

References

[1] M. Vukobratovic, A. A. Frank, and D. Jricic, **"On The Stability of Biped Locomotion",** *IEEE Trans. On Biomedical Engineering*, BME 17-1, pp. 25-36, 1970.

[2] M. Vukobratovic, and B. Brovac, **"Zero-Moment Point-Thirty five years of its life",** *Int. Journal of Humanoid Robotics*, Vol.1, No. 1, pp. 157-173, 2004.

[3] A. Goswami, **"Foot-Rotation indicator (FRI) point: A New Gait Planning Tool to Evaluate Postural Stability of Biped Robots",** *Proc. IEEE ICRA*, Detroit, pp. 47-52, 1999.

[4] A. Goswami, and V. Kallem, **"Rate of Change of Angular Momentum and Balance Maintenance of Biped Robots",** *Proc. IEEE ICRA*, New Orleans, pp. 3785-3790, 2004.

[5] H. O. Lim and A. Takanishi, **"Compensatory Motion Control for a Biped Walking Robot",** *Robotica*, Vol. 23, pp. 1-11, 2005.

[6] M. Vukobratovic et al, *Biped Locomotion Dynamic, Stability, Control and Application*, springer-verlag 1990.

[7] S. Tzafestas, M. Raibert and C. Tzafestas, **"Robust sliding-mode control applied to a 5-link biped robot",** *Int. Journal of Intelligent and Robotic Systems*, Vol.15, pp. 67–133, 1996.

[8] H. K. Lum, M.Zribi and Y. C. Soh, **"Planing and Control of a Biped Robot",** *Int. Journal of Engineering Science,* Vol.37, pp. 1319-1349, 1999.

[9] K. Mitobe, G. Capi and Y. Nasu, **"Control of walking robots based on manipulation of the zero moment point",** *Robotica*, Vol.18, pp. 651–657, 2000.

[10] K. Mitobe, N. Mori, K. Aida and Y. Nasu, **"Nonlinear feedback control of a biped walking robot",** *Proc of IEEE Int. Conf. on Robotics and Automation*, Nagoya, pp. 2865–2870, 1995.

[11] C. Chevallereau, **"Time-scaling control of an underactuated biped robot",** *IEEE Trans. on Robotics and Automation*, Vol.19, Issue.2, pp. 362–368, 2003.

[12] C. M. Chew and Gl. A. Pratt, **"A Minimum Model Adaptive Control approach for a Planner Biped",** *Int. Conf. on Intelligent Robotics and System*, Vol.3, pp. 1469-1474, 1999.

[13] X. Mu and Q. Wuy, **"Development of a complete dynamic model of a planar five-link biped and sliding mode control of its locomotion during the double support phase",** *Int. Journal of Control*,

Vol.77, No.8, pp. 789–799, 2004.

[14] S. Ali A. Moosavian, Amir Takhmar, and Mansoor Alghoneh, **"Regulated Sliding Mode Control of a Biped Robot",** *Proc. of the IEEE International Conference on Mechatronics and Automation (ICMA 2007)*, Harbin, China, August, 2007.

[15] J.E. Slotine and W. Li, *Applied Nonlinear Control*, Prentice-Hall, Englewood Cliffs, New Jersey, 1991.

[16] M. R. Rafimanzelat and M. J. Yazdanpanah, **"A novel low chattering sliding mode controller",** *Proc. of Asian Control Conference*, Vol.3, pp. 1958-1963, 2004.

[17] I. G. Park and J. G. Kim, **"Robust Control for Dynamic Walking of a Biped Robot with Ground Contacting Condition",** *Proc. ISIE,* Pusan, Vol.3, pp. 2067-2072, 2001.

[18] S. Ali. A. Moosavian, and M. Reza Homaeinejad, **"Control of Space Free-Flying Robots Using Regulated Sliding Mode Controller,"** *Proc. Of the IEEE/RSJ International Conference on Intelligent Robots and Systems (IROS 2006)*, Oct. 9-15, 2006, Beijing, China.

[19] S. Ali. A. Moosavian, and M. Reza Homaeinejad, **"Regulated Sliding Mode Control of Satellite Rotation,"** *Proc. Of the IFAC Workshop on Generalized Solutions in Control Problems (GSCP-2004)*, Russia, 22-26 Sept. 2004.

[20] R. Guclu, **"Sliding Mode and PID Control of a structural system against earthquake",** *Mathematical and Computer Modelling*, Vol.44, pp. 210-217, 2006.

[21] J. X. Xu, Y. J. Pan and T. H. Lee, **"Sliding Mode Control with closed loop filtering architecture for a class of nonlinear system",** *IEEE Trans. On Circuits and system II,* Vol.51, Issue 4, pp. 168-173, 2004.

[22] S. J. Huang and K. C. Chiou, **"An Adaptive Neural Sliding Mode Controller for MIMO Systems",** *Int. Journal of Intelligent and Robotic Systems,* Vol.46, pp. 285–301, 2006.

[23] Qi. Zhen, J.E. McInroy and F. Jafari, **"Trajectory Tracking with Parallel Robots Using Low Chattering, Fuzzy Sliding Mode Controller",** *Int. Journal of Intelligent and Robotic Systems*, Vol.48, pp. 333–356, 2007.

[24] J. H. Mathews and K. D. Fink, *Numerical Methods Using MATLAB*, Third Editon, Prentice Hall 1999.

[25] S. K. Saha, and J. Angeles, **"Dynamics of Nonholonomic Mechanical Systems Using a Natural Orthogonal Complement",** *Trans. of the ASME*, Vol. 58, pp. 238-244, March 1991.

[26] K. M. Passino and S. Yurkovich, *Fuzzy Control*, Aaddison Wesley Longman, 1998.